J Mater Sci: Mater Med (2011) 22:1985–1992
DOI 10.1007/s10856-011-4363-y

Electrodeposition of chitosan-glucose oxidase biocomposite onto Pt–Pb nanoparticles modified stainless steel needle electrode for amperometric glucose biosensor

Meiqing Guo · Haidong Fang · Rui Wang · Zhiqiang Yang · Xinhua Xu

Received: 6 April 2011 / Accepted: 28 May 2011 / Published online: 14 June 2011

Abstract A glucose biosensor was fabricated by electrodepositing chitosan (CS)-glucose oxidase(GOD) biocomposite onto the stainless steel needle electrode (SSN electrode) modified by Pt–Pb nanoparticles (Pt–Pb/SSN electrode). Firstly, Pt–Pb nanoparticles were deposited onto the SSN electrode and then CS-GOD biocomposite was co-electrodeposited onto the Pt–Pb/SSN electrode in a mixed solution containing p-benzoquinone (p-BQ), CS and GOD. The electrochemical results showed that the Pt–Pb nanoparticles can accelerate the electron transfer and improve the effective surface area of the SSN electrode. As a result, the detection range of the proposed biosensor was from 0.03 to 9 mM with a current sensitivity of 0.4485 μA/mM and a response time of 15 s. The Michaelis constant value was calculated to be 4.9837 mM. The cell test results indicated that the electrodes have a low cytotoxicity. This work provided a suitable technology for the fabrication of the needle-type glucose biosensor.

1 Introduction

Diabetes mellitus has become a worldwide public health problem. It is one of the most prevalent and costly diseases in the world [1]. Therefore, continuous monitoring of blood glucose levels becomes indispensable test for the diagnosis and management of diabetes mellitus. Although a number of routes to monitor the biological systems have been developed [2], the enzyme-based glucose biosensors have attracted special interest for researchers owing to their practical advantages, such as operation simplicity, lower expense of fabrication, higher selectivity and suitability for real time detection [3–6]. Shichiri et al. [7] achieved the purpose by using the needle-type glucose sensor with biocompatible membranes for the first time. The needle-type enzyme electrodes have been widely used for the measurement of glucose [8–10]. However, both the sensitivity and detection range for the needle-type enzyme electrode with small surface area are required to be improved and expanded.

The development of simple and reliable procedures to immobilize and stabilize reactive enzymes on the electrode has received considerable attention [11–15]. The ideal immobilization process should be cheap, quick, and enzyme friendly. Chitosan (CS) is a non-acetylated or partially deacetylated chitin. It owns many primary amino groups, and has a 6.3 of pKa [16, 17]. At pH sufficiently below the pKa, CS exists as a water-soluble cationic polyelectrolyte, since most of the amino groups are protonated. When the solution pH is raised near or above the pKa, many of the amino groups are deprotonated, and then CS becomes insoluble. Chitosan has been used as one of the most promising matrix for enzyme immobilization due to its desirable properties, such as biocompatibility, non-toxicity and excellent film-forming ability [18–20].

Electrochemical deposition has been reported recently as a simple method suitable for selective deposition of films with controllable thickness [21, 22]. Usually, electrochemical deposition of CS is performed via water reduction [6, 23, 24]. At a reducing potential, by using the

Meiqing Guo and Haidong Fang contributed equally to this work.

M. Guo · H. Fang · R. Wang · Z. Yang · X. Xu (✉)
School of Materials Science and Engineering,
Tianjin University, Tianjin 300072, China
e-mail: xhxu_tju@eyou.com

X. Xu
Tianjin Key Laboratory of Composite and Functional Materials,
Tianjin 300072, China

locally generated H^+ gradient, acidic side chains of CS are titrated and then the solubility of CS changes, eventually leading to the controlled deposition of CS film. Meanwhile, other substances such as enzymes [25] could be effectively entrapped into CS film during the electrodeposition. However, for the reported CS-electrodeposition protocols via water reduction, high voltage or high current densities must be applied to promote the proton consumption on the electrode surface [24]. Enzyme in solution might partially denaturalize or lose activity at such high potential or current density. Zhou et al. [26] reported that some deliberately p-benzoquinone (p-BQ) could be used as a "proton-consume" instead of water. By this means, the electrochemically deposited CS can be carried out under much milder conditions.

However, the previous researches about electrochemical deposition of CS-based composite were all performed on the flat electrode. There were no works reported on the electrochemical deposition of CS-based composite onto Pt–Pb nanoparticles modified stainless steel needle electrode. Compared with the flat electrode, nanoparticles modified electrodes exhibited many attractive characteristics such as large active surface area and small charge-transfer resistance [27]. In addition, the electrical contact between the redox center of GOx and electrode supports can be improved by using nanomaterials [28]. Thus the electrochemical signal on the electrode modified by nanoparticles would be increased, which was significant for fabricating the biosensors.

Accordingly, in the present study, combining the advantageous features of Pt–Pb nanoparticles and electrochemical deposition, we presented a glucose biosensor fabricated by electrodepositing chitosan-glucose oxidase biocomposite onto Pt–Pb nanoparticles modified stainless steel needle electrode. The morphology and microstructure of Pt–Pb nanoparticles were then investigated by field-emission scanning electron microscope (FE-SEM), X-ray diffraction (XRD), X-ray photoelectron spectroscopy (XPS) and energy dispersive X-ray detector (EDX). Cyclic voltammetrys (CVs), response time, linear range, detection limit, current sensitivity, the Michaelis constant and cytotoxicity were used to characterize the proposed glucose biosensor.

2 Materials and methods

2.1 Reagents

Chitosan (CS) (95% deacetylated) and GOD (E.C.1.1.3.4, 21.1 unit/mg) were purchased from Sigma. $H_2PtCl_6{\cdot}6H_2O$ was purchased from Aldrich. Glucose, hydrochloric acid, p-benzoquinone (p-BQ) and lead acetate $Pb(CH_3COO)_2$ were purchased from Kewei Chemical Reagent Co Ltd of Tianjin University (Tianjin, China). All other chemicals were of analytical grade and used without further purification. 0.5% CS solution was prepared by dissolving CS solid in 0.1 M acetic acid (HAc). The pH of the solution was adjusted to 5.0 via careful additions of concentrated NaOH under vigorous stirring. Phosphate buffer solution (PBS, 0.2 M) consisted of Na_2HPO_4 and NaH_2PO_4 was employed as the supporting electrolyte. All aqueous solution was prepared with doubly distilled water. All experiments were performed in PBS at room temperature (25°C).

2.2 Instruments

All the electrochemical measurements were performed on PARSTAT 2263 electrochemical workstation (Princeton, USA). A conventional three-electrode system was used with the SSN electrode or the Pt–Pb/SSN electrode (0.35 mm in diameter) as a working electrode, a platinum electrode (1 mm in diameter) as an auxiliary electrode and a saturated calomel electrode (SCE) as a reference electrode in all cases. Electrochemical impedance spectroscopy (EIS) measurements were performed at open circuit potentials in 1 M KCl containing 5.0 mM $K_3Fe(CN)_6$/$K_4Fe(CN)_6$ (1:1) mixture with the frequencies ranging from 100 kHz to 10 mHz. The morphology and composition of the Pt–Pb nanoparticles were analyzed by SEM (S-4800, Hitachi, Japan), XPS (PHL1600ESCA XPS), XRD (RIGAKU/DMAX2500, Japan) and EDX (Genesis XM2 APEX 60SEM, EDAX, USA).

2.3 Preparation of the GOD-CS/Pt–Pb/SSN electrode

Figure 1 showed the scheme for fabricating the GOD-CS/Pt–Pb/SSN electrode. Prior to the electrodeposition, the SSN electrode was electrochemically pretreated by cyclic potential scanned from −0.4 to 0.6 V (vs. SCE) at a scan rate of 50 mV/s until CVs became reproducible. Then, the electrodeposition of Pt–Pb nanoparticles onto the SSN electrode was carried out in 0.5 M HCl solution containing 2.5 mg/ml H_2PtCl_6 and 1.85 mg/ml $Pb(CH_3COO)_2$ at 10 mA for 20 min with ultrasonication. The electrodeposition of GOD-CS was triggered by reduction of p-BQ at −0.1 V (vs. SCE) for 300 s in 0.5% CS solution containing

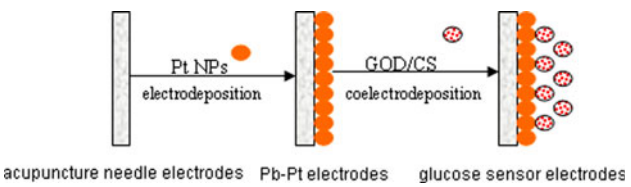

Fig. 1 Schematic diagram of the fabrication of the GOD-CS/Pt–Pb/SSN electrode

20 mM p-BQ and 5 mg/ml GOD. When not in use, the prepared electrodes were stored in refrigerator (4°C).

2.4 Cell viability assay

Mouse fibroblast cell (L929) purchased from Peking Union Medical College (Beijing, China) was incubated in Dulbecco's Modified Eagle's Medium (DMEM) containing 10% fetal bovine serum (FBS), 100 units/ml penicillin and 100 mg/ml streptomycin at 37°C in 5% CO_2 humidified atmosphere.

The MTT assay was used to determine the cytotoxicity. The method was carried out with the immersion extracts in contact with L929. To prepare extracts, each sample was sterilized by ^{60}Co radiation and then incubated in each well for 24 h before refreshing the medium with fresh complete medium (200 ml/well). L929 cells were seeded in a 96-well plate at 2×10^4 cells/well and incubated for 24 h at 37°C in 5% CO_2 humidified atmosphere. Then, the culture medium was removed and replaced by the immersion extracts. After incubation for 24 h, 20 ml/well MTT (5 mg/ml in PBS) was added to each well, and the plate was further incubated for 4 h. Then, all media were removed and 150 ml/well dimethylsulfoxide (DMSO) was added, followed by shaking for 10 min. The absorbance of each well was measured at 570 nm on a $\sum$960 plate-reader (Metertech) with pure DMSO as a blank. Non-treated cell (in DMEM) was used as a control and the relative cell viability (mean% $\pm$ SD, $n = 3$) was expressed as ODsample/ODcontrol $\times$ 100%.

3 Results and discussion

3.1 Characterization of Pt–Pb/SSN electrode

The merit of electrodeposition method for fabricating Pt–Pb/SSN electrode was easy to control the size and density of particles by varying the electrodeposition conditions such as the electrolyte concentration, the deposition current and time. It was found that uniform Pt–Pb nanoparticles on the SSN electrode and excellent electrochemical performance of Pt–Pb/SSN electrode were obtained when 10 mA, 20 min and 2.5 mg/ml were used as the electrodeposition conditions. The composition and morphology of the SSN electrode and Pt–Pb/SSN electrode were determined by SEM and EDX, and typical images were presented in Figs. 2 and 3. From EDX spectrum in Fig. 2b, the element of Pt and Pb can be observed, and the atom ratio of Pt/Pb was 37.48:43.05. From Fig. 3a, b, it was observed that the surface roughness of SSN electrode was increased obviously. From Fig. 3a, it can be found that the average particle size of the Pt–Pb nanoparticles deposited on the surface of the SSN electrode was in the range of 200–300 nm. As seen in Fig. 3c, the average thickness of Pt–Pb film was at about 100 nm.

The surface composition of Pt–Pb nanoparticles was further characterized by XPS. Figure 2c, d showed the XPS spectra of the Pt 4f (c) and Pb 4f (d) regions for the Pt–Pb nanoparticles, respectively. The binding energy of Pt 4f was observed at approximately 71.4 and 74.7 eV, which was assigned to the metallic Pt. The binding energy of Pb 4f was 136.6 and 141.7 eV. The peak at 136.6 and 141.7 eV were in good agreement with the metallic Pb. The results indicated that Pt and Pb were in their alloy form coexistent in the Pt–Pb nanoparticles.

The structure of Pt–Pb nanoparticles was investigated by XRD. Figure 2e showed XRD patterns of the Pt–Pb nanoparticles. As observed in Fig. 2e, the peaks around 38.44°, 44.84° and 65.14° were observed, which were due to the PbPtx (1 1 1) (2 0 0) and (2 2 0), respectively [29].

3.2 Electrochemical characterization of Pt–Pb/SSN electrode

3.2.1 Impedance analysis of Pt–Pb/SSN electrode

EIS was a well-known effective method for studying the interface properties [30]. Figure 4 showed the typical EIS of the bare SSN electrode and Pt–Pb/SSN electrode. Significant differences in the impedance spectra were observed. For the bare SSN electrode, only the high frequency arc was observed, which indicated that the bare SSN electrode showed typical resistance characteristics and no capacitive characteristics. For the Pt–Pb/SSN electrode, the impedance spectra followed the theoretical shapes, a squeezed semicircle observed at high frequency, which corresponded to the electron transfer limited process, followed by a linear part at the low frequency attributable to diffusion controlled electron transfer process. In the low frequency region, no vertical increase in impedance on the imaginary part with decreasing the ac frequency was observed, which demonstrated that the Pt–Pb/SSN electrode showed no capacitive characteristics.

The respective semicircle diameters at the high frequency, equalled to the electron transfer resistance (Rct) at the electrode surface. From Fig. 4, it can be seen that the Rct of the Pt–Pb/SSN electrode was estimated to be 100 Ω, noticeably smaller than 1800 kΩ of the SSN electrode. The results indicated that the Pt–Pb nanoparticles deposited on the electrode can play an important role similar to electron-conducting tunnel, which made it easier for the electron transfer to take place.

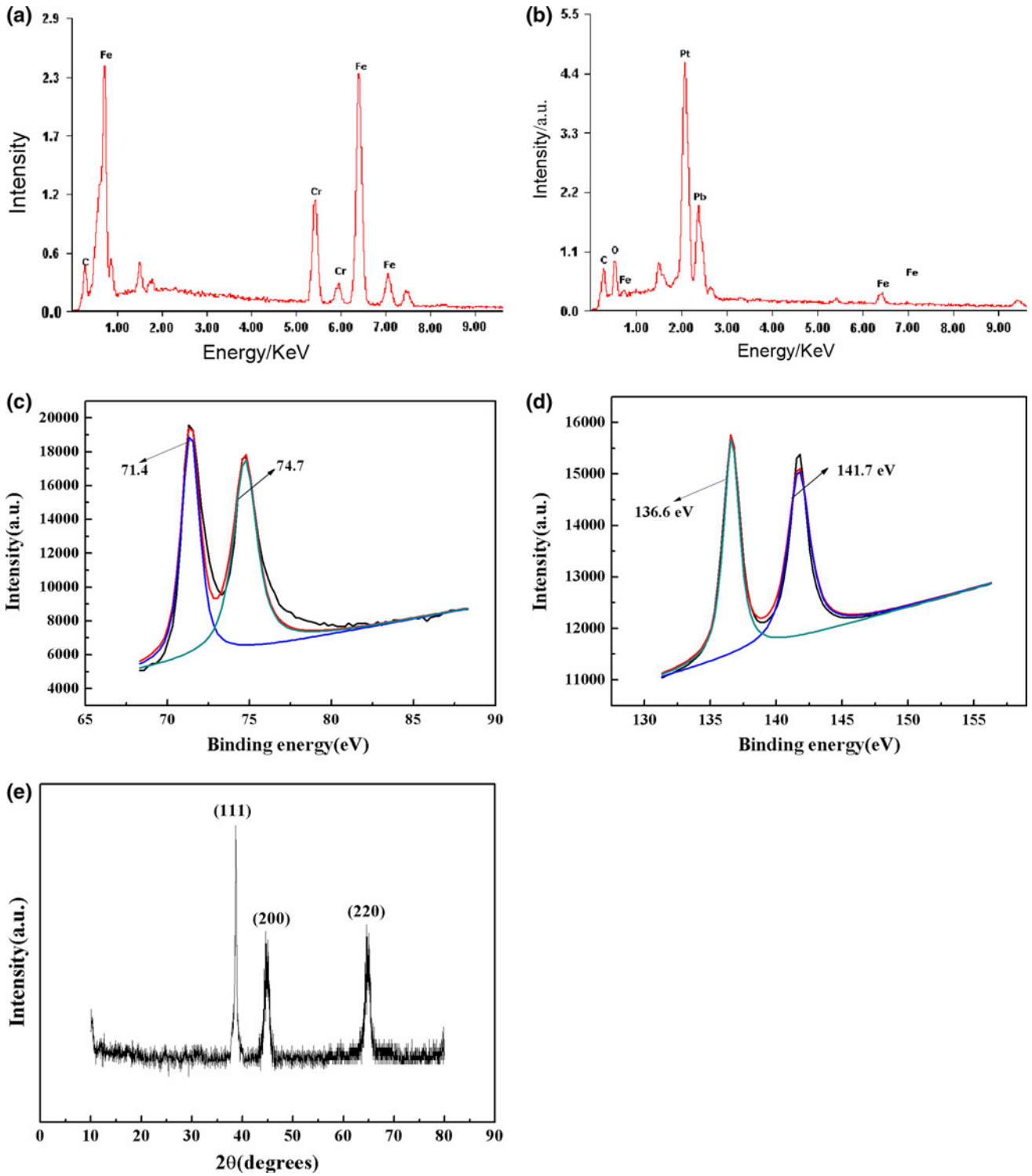

Fig. 2 EDX spectrum of the SSN electrode (**a**) and the Pt–Pb/SSN electrode (**b**); XPS spectra of the Pt 4f (**c**) and Pb 4f (**d**) regions for the Pt–Pb nanoparticles; **e** XRD patterns of the Pt–Pb nanoparticles

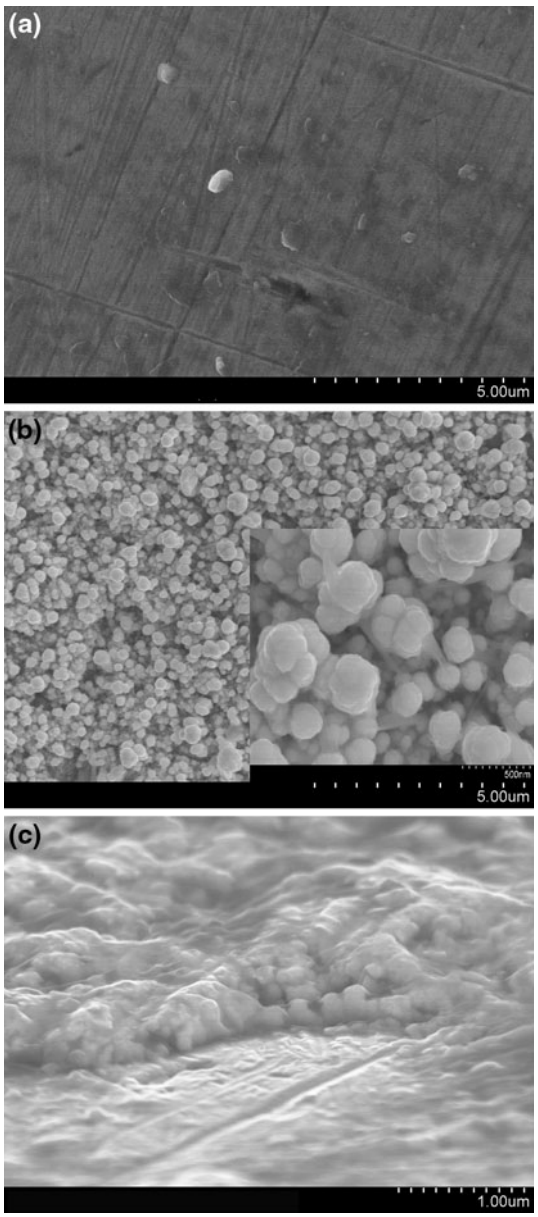

Fig. 3 Top SEM images of the SSN electrode (**a**) and Pt–Pb/SSN electrode (**b**) and the cross section image of the Pt–Pb/SSN electrode (**c**). *Inset* of the Fig. 3b is the magnified image of the Pt–Pb/SSN electrode

3.2.2 *Determination of the effective surface area of the Pt–Pb/SSN electrode*

The electroactive surface area of the Pt–Pb/SSN electrode was estimated by CVs using $K_3[Fe(CN)_6]$ as an electrochemical probe. Figure 5 displayed CVs on the Pt–Pb/SSN electrode at different scan rates in 5 mM $K_3Fe(CN)_6$ solution with 1 M KCl as supporting electrolyte. From Fig. 5, the dependence of the peak current (I_{pa} or I_{pc}) on the square root of the potential scan rate ($v^{1/2}$) was described by the following equation:

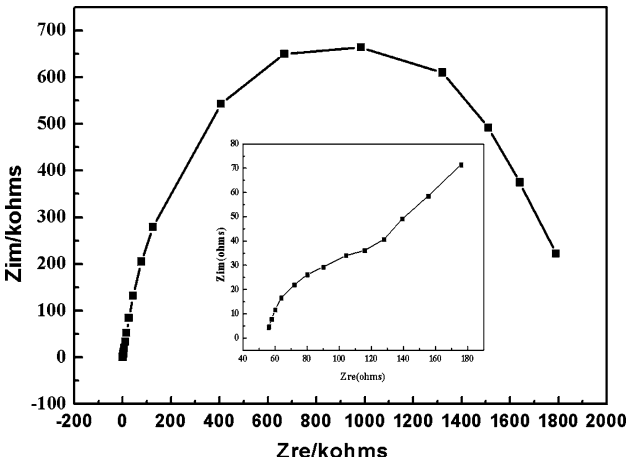

Fig. 4 Electrochemical impedance spectra of the SSN electrode and (*Inset*) the Pt–Pb/SSN electrode in 1 M KCl solution containing 5 mM $[Fe(CN)^6]^{3-/4-}$

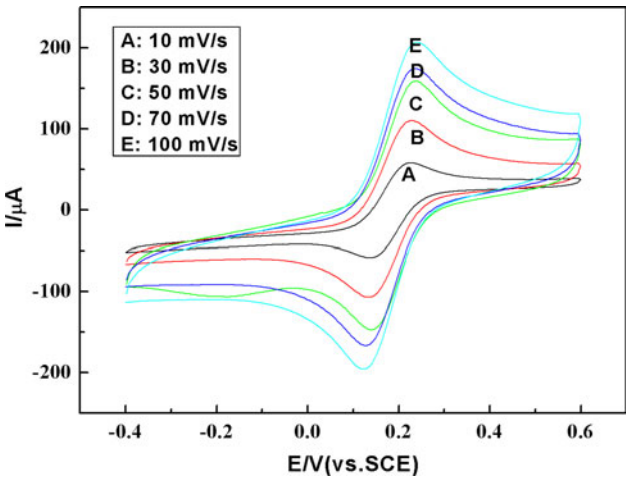

Fig. 5 CVs of the Pt–Pb/SSN electrode in 1 M KCl solution containing 5 mM $K_3[Fe(CN)_6]$ at different scan rates (from inner to outer): 10, 30, 50, 70, 100 mV/s

$$Ip/(\mu A) = 21.88 \pm 0.081 v^{1/2}/(V/s) - 6.69 \pm 0.573 (R = 0.999) \quad (1)$$

The peak current (*Ip*) increased linearly with the square root of the potential scan rate ($v^{1/2}$), which suggested that the reaction occurred on the modified electrode was nearly reversible. The results also illustrated that the mass transfer phenomenon in the double layer region of the electrode was mainly diffusion controlled [31]. The effective surface area (A) can be calculated from the following Randles–Sevcik equation [32]:

$$Ip = 0.4463 \left(F^3/RT\right)^{1/2} n^{3/2} A_0 D_0^{1/2} C_0 v^{1/2} \quad (2)$$

where n represents the number of electrons participating in the redox reaction, v is the scan rate of the potential perturbation (V/s), A_0 (cm^2), D_0 ($7.6 \times 10^{-6} cm^2/s$),

C_0 (mol/cm^3), refer to the area, diffusion coefficient and concentration of species O, respectively. For T = 298 K (25°C), one has: $0.4463(F^3/RT)^{1/2} = 2.687 \times 10^5$ As/(mol $V^{1/2}$). *Ip* is the peak current in CVs illustrated in the inset of Fig. 5. According to these, the calculated effective working area of the Pt–Pb/SSN electrode was 0.189 cm^2.

3.2.3 *Cyclic voltammetrys behavior of the Pt–Pb/SSN electrode*

The CVs were used to characterize the electrochemical behavior of the Pt–Pb/SSN electrode. From Fig. 6, the dependence of the peak current (I_{pa} or I_{pc}) on the scan rate (v) were described by the following equations:

$$I_{pa}/(\mu A) = 3.795 \pm 0.1854v/(mV/s) + 58.98 \pm 11.60(R = 0.999) \quad (3)$$

$$I_{pc}/(\mu A) = -3.8204 \pm 0.3002v/(mV/s) - 87.13 \pm 18.60(R = 0.999) \quad (4)$$

Form the above equations, it can be seen that with scan rate from 10 to 100 mV/s, the anodic and cathodic peak currents increased linearly, indicating a surface-controlled process [33, 34].

3.3 Amperometric determination of glucose with the biosensor

Figure 7 illustrated current–time plots for the GOD-CS/Pt–Pb/SSN electrode under the optimized experimental conditions with successive additions of glucose into PBS. The sensor displayed a high sensitivity of 0.4485 μA/mM and a fast response time of only 15 s. The Pt–Pb nanoparticles on the SSN electrode provided big surface area, good conductivity, and catalytic activity. Therefore, many

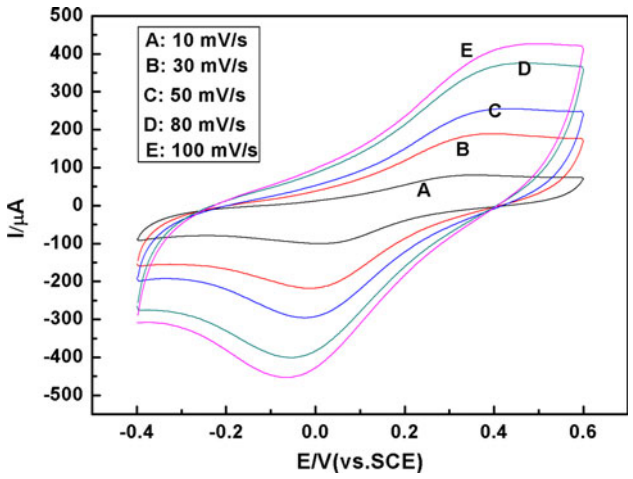

Fig. 6 CVs of the Pt–Pb/SSN electrode in the 7.0 PBS solution at different scan rates: (from inner to outer): 10, 30, 50, 80 and 100 mV/s

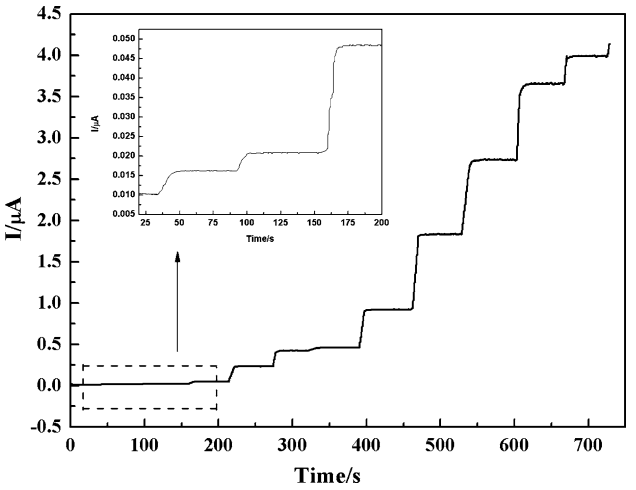

Fig. 7 Amperometric response of the GOD-CS/Pt–Pb/SSN electrode to successive injection of glucose in a stirred 30 ml 7.0 PBS solution at 0.3 V (vs SCE). Inset is the enlarged drawing of the Fig. 7 in the range of the lower glucose concentration

of GOD molecules incorporated with CS can be located on the electrode, and consequently a sensitive catalytic current to glucose was obtained. The calibration curve of the GOD-CS/Pt–Pb/SSN electrode was described by the following equation:

$$I/(\mu A) = 0.4485 \pm 0.0034 Cglucose/(mM) + 0.011 \pm 0.0144(R = 0.9995) \quad (5)$$

The GOD-CS/Pt–Pb/SSN electrode displayed an expanded linear detection glucose concentration range from 0.03 to 9 mM with the current sensitivity was 0.4485 μA/mM ($n = 11$) to glucose. The high sensitivity at the GOD-CS/Pt–Pb/SSN electrode would be resulted from the large active surface area and the excellent electron-transfer ability of the Pt–Pb/SSN electrode. The apparent Michaelis–Menten constant (K_M^{app}) can be calculated from the electrochemical version of the Linweaver–Burk equation:

$$1/I_{ss} = 1/I_{max} + K_M^{app}/(Cglucose \cdot I_{max}) \quad (6)$$

where I_{ss} is the steady-state current after the addition of substrate, I_{max} is the maximum current under saturated substrate conditions, Cglucose is the concentration of glucose. According to the calibration curve, the Linweaver–Burk equation can be described by the equation:

$$1/I_{ss}/(\mu A) = 1.8759 \pm 0.0208/Cglucose/(mM) + 0.3764 \pm 0.2702(R = 0.999) \quad (7)$$

The K_M^{app} value for the GOD-CS/Pt–Pb/SSN electrode was found to be 4.9837 mM. The smaller K_M^{app} value meant that GOD entrapped in the CS exhibited high enzymatic activity and affinity to glucose.

3.4 Cell viability evaluation

To evaluate the cytotoxicity of the electrode, the MTT assay method was used to determine the relative cell viability. That was, only alive mitochondria can oxidize MTT, generating a typical blue formazan reaction product. This assay was an indirect method for testing cell viability and proliferation since the absorbance at 570 nm depending on the cell number. The relative cell viability (% of control) was calculated to be 93 ± 5%, which indicated that the electrodes exhibited a low cytotoxicity.

4 Conclusions

In the present work, a glucose biosensor was fabricated by electrodepositing chitosan-glucose oxidase biocomposite onto Pt–Pb/SSN electrode. The results revealed that the Pt–Pb nanoparticles were composed of PbPtx (the atom ratio of Pt/Pb was 37.48:43.05), and Pt and Pb were in their alloy form coexistent in the Pt–Pb nanoparticles. The electrochemical results showed that the Pt–Pb nanoparticles can accelerate the electron transfer and improve the effective surface area of the SSN electrode. The linear detection range of the proposed biosensor was from 0.03 to 9 mM with a current sensitivity of 0.4485 μA/mM and a response time of 15 s. The Michaelis constant value was calculated to be 4.9837 mM. The cell test results showed that the electrodes have a low cytotoxicity. The present work demonstrated that the Pt–Pb nanoparticles can improve the amperometric current of the SSN electrode with small surface area.

Acknowledgment The authors gratefully acknowledge the financial support of the Natural Science Foundation of Tianjin in China (08JC2DJC17900).

References

1. Pei JH, Tian F, Thundat T. Glucose biosensor based on the microcantilever. Anal Chem. 2004;76:292–7.
2. Wilson GS, Hu YB. Enzyme based biosensors for in vivo measurements. Chem Rev. 2000;100:2693–704.
3. Zhao W, Xu JJ, Shi CG, Chen HY. Multilayer membranes via layer-by-layer deposition of organic polymer protected Prussian blue nanoparticles and glucose oxidase for glucose biosensing. Langmuir. 2005;21:9630–4.
4. Wang G, Mantey K, Nayfeh MH, Yau ST. Enhanced amperometric detection of glucose using Si-29 particles. Appl Phys Lett. 2006;89:243901.
5. Wang G, Yau ST, Mantey K, Nayfeh MH. Fluorescent Si nanoparticle-based electrode for sensing biomedical substances. Opt Commun. 2008;281:1765–70.
6. Wu BY, Hou SH, Yin F, Zhao ZX, Wang YY, Wang XS, Chen Q. Amperometric glucose biosensor based on multilayer films via layer-by-layer self-assembly of multi-wall carbon nanotubes, gold nanoparticles and glucose oxidase on the Pt electrode. Biosens Bioelectron. 2007;22:2854–60.
7. Ahmed S, Dack C, Farace G, Rigby G, Vadgama P. Tissue implanted glucose needle electrodes: early sensor stabilisation and achievement of tissue-blood correlation during the run in period. Anal Chim Acta. 2005;537:153–61.
8. Churchouse SJ, Battersby CM, Mullen WH, Vadgama PM. Needle enzyme electrodes for biological studies. Biosens Bioelectron. 1986;2:325–42.
9. Ichimori S, Nishida K, Shimoda S, Sekigami T, Matsuo Y, Ichinose K, Shichiri M, Sakakida M, Araki E. Development of a highly responsive needle-type glucose sensor using polyimide for a wearable artificial endocrine pancreas. J Artif Organs. 2006;9:105–13.
10. Shen J, Dudik L, Liu CC. An iridium nanoparticles dispersed carbon based thick film electrochemical biosensor and its application for a single use, disposable glucose biosensor. Sensor Actuat B-Chem. 2007;125:106–13.
11. Chen Q, Kobayashi Y, Takeshita H, Hoshi T, Anzai J. Avidin-biotin system-based enzyme multilayer membranes for biosensor applications: optimization of loading of choline esterase and choline oxidase in the bienzyme membrane for acetylcholine biosensors. Electroanalysis. 1998;10:94–7.
12. Hoshi T, Saiki H, Kuwazawa S, Tsuchiya C, Chen Q, Anzai J. Selective permeation of hydrogen peroxide through polyelectrolyte multilayer films and its use for amperometric biosensors. Anal Chem. 2001;73:5310–5.
13. Ammam M, Fransaer J. Two-enzyme lactose biosensor based on beta-galactosidase and glucose oxidase deposited by AC-electrophoresis: characteristics and performance for lactose determination in milk. Sensor Actuat B-Chem. 2010;148:583–9.
14. Ammam M, Fransaer J. AC-electrophoretic deposition of glucose oxidase. Biosens Bioelectron. 2009;25:191–7.
15. Ammam M, Fransaer J. AC-electrophoretic deposition of glucose oxidase (vol 25, pg 191, 2009). Biosens Bioelectron. 2010;25:1856–1856.
16. Sorlier P, Denuziere A, Viton C, Domard A. Relation between the degree of acetylation and the electrostatic properties of chitin and chitosan. Biomacromolecules. 2001;2:765–72.
17. Wang XY, Gu HF, Yin F, Tu YF. A glucose biosensor based on Prussian blue/chitosan hybrid film. Biosens Bioelectron. 2009;24:1527–30.
18. Chen X, Jia JB, Dong SJ. Organically modified sol-gel/chitosan composite based glucose biosensor. Electroanalysis. 2003;15:608–12.
19. Wang G, Xu JJ, Chen HY, Lu ZH. Amperometric hydrogen peroxide biosensor with sol-gel/chitosan network-like film as immobilization matrix. Biosens Bioelectron. 2003;18:335–43.
20. Cao SS, Mishra R, Pilla S, Tripathi S, Pandey MK, Shah G, Mishra AK, Prabaharan M, Mishra SB, Xin J, Pandey RR, Wu WW, Pandey AC, Tiwari A. Novel chitosan/gold-MPA nanocomposite for sequence-specific oligonucleotide detection. Carbohyd Polym. 2010;82:189–94.
21. Bharathi S, Nogami M, Ikeda S. Novel electrochemical interfaces with a tunable kinetic barrier by self-assembling organically modified silica gel and gold nanoparticles. Langmuir. 2001;17:1–4.
22. Deepa PN, Kanungo M, Claycomb G, Sherwood PMA, Collinson MM. Electrochemically deposited sol-gel-derived silicate films as a viable alternative in thin-film design. Anal Chem. 2003;75:5399–405.
23. Yi HM, Wu LQ, Ghodssi R, Rubloff GW, Payne GF, Bentley WE. A robust technique for assembly of nucleic acid hybridization chips based on electrochemically templated chitosan. Anal Chem. 2004;76:365–72.
24. Yi HM, Wu LQ, Ghodssi R, Rubloff GW, Payne GF, Bentley WE. Signal-directed sequential assembly of biomolecules on patterned surfaces. Langmuir. 2005;21:2104–7.

25. Xi FN, Liu LJ, Wu Q, Lin XF. One-step construction of biosensor based on chitosan-ionic liquid-horseradish peroxidase biocomposite formed by electrodeposition. Biosens Bioelectron. 2008; 24:29–34.
26. Zhou QM, Xie QJ, Fu YC, Su ZH, Jia X, Yao SZ. Electrodeposition of carbon nanotubes-chitosan-glucose oxidase biosensing composite films triggered by reduction of p-benzoquinone or H_2O_2. J Phys Chem B. 2007;111:11276–84.
27. Li C, Liu Y, Luong JHT. Impedance sensing of DNA binding drugs using gold substrates modified with gold nanoparticles. Anal Chem. 2005;77:478–85.
28. Wang J. Electrochemical glucose biosensors. Chem Rev. 2008; 108:814–25.
29. Sun YP, Buck H, Mallouk TE. Combinatorial discovery of alloy electrocatalysts for amperometric glucose sensors. Anal Chem. 2001;73:1599–604.
30. Shervedani RK, Mehrjardi AH, Zamiri N. A novel method for glucose determination based on electrochemical impedance spectroscopy using glucose oxidase self-assembled biosensor. Bioelectrochemistry. 2006;69:201–8.
31. Miao XM, Yuan R, Chai YQ, Shi YT, Yuan YY. Direct electrocatalytic reduction of hydrogen peroxide based on Nafion and copper oxide nanoparticles modified Pt electrode. J Electroanal Chem. 2008;612:157–63.
32. Song MJ, Hwang SW, Whang D. Non-enzymatic electrochemical CuO nanoflowers sensor for hydrogen peroxide detection. Talanta. 2010;80:1648–52.
33. Laviron E, Roullier L. Electrochemical reactions with adsorption of the reactants and electrosorption. Simple analytical solutions for a Henry isotherm. J Electroanal Chem. 1998;443:195–207.
34. Laviron E. General expression of the linear potential sweep voltammogram in the case of diffusionless electrochemical systems. J Electroanal Chem. 1979;101:19–28.